Quantitative Evaluation of Sensor Fault Diagnosability of F-16 High Maneuvering Fighter

Zili Wang
College of Automation
Nanjing University of Aeronautics and Astronautics
Nanjing, China
wangzili@nuaa.edu.cn

Zihui Tang
College of Automation
Nanjing University of Aeronautics and Astronautics
Nanjing, China
tangzihui@nuaa.edu.cn

Fuyang Chen
College of Automation
Nanjing University of Aeronautics and Astronautics
Nanjing, China
chenfuyang@nuaa.edu.cn

2022 IEEE 5th International Conference on Automation, Electronics and Electrical Engineering (AUTEEE) | 978-1-6654-7197-8/22/$31.00 ©2022 IEEE | DOI: 10.1109/AUTEEE56487.2022.9994383

***Abstract*—Due to the nonlinear and fast time-varying characteristics, the fault diagnosability of the F-16 fighter has become a rigorous performance index. In this paper, a quantitative fault diagnosability evaluation method of nonlinear system based on adaptive kernel density estimation (AKDE) and Jensen Shannon (JS) divergence is proposed. The affine nonlinear model of F-16 inner loop with sensor fault and aerodynamic parameter variation is considered. The probability density function (PDF) of sensor output residual under fault and normal conditions is estimated by KDE, and the adaptive bandwidth is designed to ensure the accuracy of PDF estimation. By introducing Monte Carlo method, the high complexity of nonlinear structure in JS divergence calculation is overcome, and the evaluation index of fault diagnosability is designed; Finally, the rationality and effectiveness of this method are verified by comparable simulation experiments.**

Keywords—F-16, JS divergence, adaptive kernel density estimation, fault diagnosability

I. INTRODUCTION

The F-16 fighter has the characteristics of fast flight speed, however the parameter uncertainty greatly increases the probability of fault occurring in the flight control system, and even leads to catastrophic accidents [1]. In this case, no matter how advanced the diagnosis algorithm is designed, the fault that cannot be diagnosed in the flight control system cannot be detected. At present, many scholars believe that fault diagnosability can describe the ability of the control system to effectively diagnose faults [2], [3], and methods such as differential geometry and coprime decomposition are applied to the evaluation. Therefore, how to evaluate the fault diagnosability of the flight control system to improve the reliability of the system in the design stage has engineering value and broad development prospects.

The fault forms studied above are all faults occurring in the dynamics system, instead of considering the faults occurring in the sensor. For the measurement error that is difficult to eliminate by the sensor, Jiang [4] calculated the allowable measurement error area of Kullback Leibler divergence (KLD) as diagnosability index by Monte Carlo method. In these studies, how to estimate the distribution function of the sensor output residual becomes the key to solve the problem of evaluating the diagnosability [5].

Nonparametric kernel density estimation (NKDE) based on probability statistics is widely used in the estimation of probability distribution model, which does not need to assume any distribution in advance and is very suitable for the feature space with random distribution [6]. Song [7] used KDE to estimate the probability density of the amplitude from the gear time-domain vibration signal. Aimed at obtaining the fault diagnosis threshold due to the uncertainty of the output distribution characteristics, Pan [8] established a probability model based on the NKDE by allocating the confidence value of the model.

Based on the above discussion, we propose a diagnosability quantitative evaluation scheme based on JS divergence and AKDE. The main contributions of this paper are as follows:

- In this paper, Monte Carlo is used to overcome the high complexity of the nonlinear structure calculation, and the fault diagnosability evaluation index is given.
- The KDE with adaptive bandwidth optimization is adopted to improve the accuracy of diagnosability evaluation.

The remainder of this paper is arranged as follows. In Section II, the affine nonlinear model of F-16 with sensor faults and aerodynamic parameter variation are established. The fault diagnosability evaluation method based on AKDE and JS divergence is constructed in Section III. Section IV verifies the correctness of the quantitative evaluation proposed in this paper. Conclusions are drawn in Section V.

II. PROBLEM DESCRIPTION

In this section, F-16 nonlinear dynamic model with sensor fault and aerodynamic parameter variation is introduced and analyzed.

A. Nonlinear dynamic model and control law

In this paper, the F-16 model is shown in (1), where x, y, z denote projections of aircraft centroid on the earth axis system, u, v, w represent speed components of airframe coordinate system, ϕ, θ, ψ, p, q, r, V, α, β express roll angle, pitch angle, yaw angle, roll angular rate, pitch angular rate, yaw angular rate, flight speed, angle of attack, sideslip angle, respectively. $c_1 \sim c_9$ stand for moment of inertia coefficient. $\bar{L}, \bar{M}, \bar{N}$ specify roll, pitch, yaw aerodynamic moment. m is aircraft mass, F_T is engine thrust, F_y, F_z are thrust of y, z axis. $g_1 \sim g_3$ correspond to gravity acceleration component. D, L, Y indicate drag, lift and side force.

The aerodynamic force and aerodynamic moment in the aerodynamic parameter model of the F-16 fighter are described as:

$$\begin{cases} \dot{x} = u\cos\psi\cos\theta + v(\cos\psi\sin\theta\sin\phi - \sin\psi\cos\phi) + w(\cos\psi\sin\theta\cos\phi + \sin\psi\sin\phi) \\ \dot{y} = u\sin\psi\cos\theta + v(\sin\psi\sin\theta\sin\phi + \cos\psi\cos\phi) + w(\sin\psi\sin\theta\cos\phi - \cos\psi\sin\phi) \\ \dot{z} = -u\sin\theta + v\cos\theta\sin\phi + w\cos\theta\cos\phi \\ \dot{\phi} = p + \tan\theta(q\sin\phi + r\cos\phi) \\ \dot{\theta} = q\cos\phi - r\sin\phi \\ \dot{\psi} = \dfrac{1}{\cos\theta}(q\sin\phi + r\cos\phi) \\ \dot{p} = c_1 qr + c_2 pq + c_3\bar{L} + c_4(\bar{N} + \bar{N}_T) \\ \dot{q} = c_5 pr - c_6(p^2 - r^2) + c_7(\bar{M} + \bar{M}_T) \\ \dot{r} = c_8 pq - c_2 qr + c_4\bar{L} + c_9(\bar{N} + \bar{N}_T) \\ \dot{V} = \dfrac{1}{m}(F_T\cos\alpha\cos\beta - D + mg_1 + F_y\sin\beta + F_z\cos\beta\sin\alpha) \\ \dot{\alpha} = (r\sin\alpha - p\cos\alpha)\tan\beta + q + \dfrac{1}{mV\cos\beta}(-L + mg_2 - F_T\sin\alpha + F_z\cos\alpha) \\ \dot{\beta} = p\sin\alpha - r\cos\alpha + \dfrac{1}{mV}(mg_3 - F_T\cos\alpha\sin\beta + Y + F_y\cos\beta + F_z\sin\beta\sin\alpha) \end{cases} \tag{1}$$

$$\begin{cases} D = \bar{q}SC_D \\ L = \bar{q}SC_L \\ Y = \bar{q}SC_Y \\ \bar{L} = \bar{q}SbC_l \\ \bar{M} = \bar{q}ScC_m \\ \bar{N} = \bar{q}SbC_n \end{cases} \tag{2}$$

C_l, C_m, C_n denotes the moment coefficients， $\bar{q} = \dfrac{1}{2}\rho V^2$, where ρ denotes the air density.

Define state variables as $x_1 = [\alpha\ \beta\ \phi]^T$, $x_2 = [p\ q\ r]^T$, control input variables as $u = [\delta_e\ \delta_a\ \delta_r\ \delta_y\ \delta_z]^T$, then the affine nonlinear model of the inner and outer loops of the system without fault is expressed as

$$\begin{cases} \dot{x}_1 = f_1(x_1) + g_1(x_1)x_2 \\ \dot{x}_2 = f_2(x_2) + g_2(x_2)u \end{cases} \tag{3}$$

where $f_1(x_1), f_2(x_2)$ denote the nonlinear dynamic coupling matrix of outer loop and inner loop, $g_1(x_1), g_2(x_2)$ denote the input distribution matrix of outer loop and inner loop, δ_e , δ_a and δ_r denote elevator, aileron and rudder respectively, δ_y is the thrust vector generated by lateral actuator, δ_z is the thrust vector generated by side actuator.

Assumption 1: The matrix $g_1(x_1), g_2(x_2)$ are non-singular.

Simplify the nominal model of the inner loop as

where C_L, C_D, C_Y denote the aerodynamic coefficients,

$$\dot{x}_2 = f_2(x_2) + g_2(x_2)u_{NDI} \tag{4}$$

(4) is reversed to provide control of surface deflection, so as to obtain the ideal control input

$$u_{NDI} = g_2^{-1}(x_2)(v_{2d} - f_2(x_2)) \tag{5}$$

The control signal of inner loop system is designed

$$v_{2d} = \begin{cases} \dot{p}_d = k_{p1}e_p \\ \dot{q}_d = k_{q1}e_q \\ \dot{r}_d = k_{r1}e_r \end{cases} \tag{6}$$

where $e_i = i_d - i$, $i = p,q,r$ are tracking errors, k_{i1}, k_{i2} , $i = p,q,r$ are control factors. Accurate tracking can be achieved by adjusting the parameters of the controller. The command inputs p_d, q_d, r_d are provided by the outputs of the outer loop system.

B. Affine nonlinear inner loop model with sensor fault

Bias fault is a common sensor fault. With (4), the attitude system model with sensor fault can be established as

$$\begin{cases} \dot{x}_2 = f_2(x_2) + g_2(x_2)u \\ y = C_2x_2 + Ff \end{cases} \tag{7}$$

where C_2 is the observation matrix, $F = \begin{bmatrix} f_p & f_q & f_r \end{bmatrix}^T$ is the bias coefficient matrix where $f_{\min} < f_i < f_{\max}\ i = p,q,r$ is a bounded variable, f indicates sensor fault.

Assumption 2: F is the column full rank matrix.

Since the actual gas effect during the large maneuvering flight lead to the change of the aerodynamic pressure distributed around the aircraft, which will cause the variation of the yaw moment, roll moment and pitch moment required by the whole flight system. Considering the variation of the roll moment coefficient C_l , pitch moment coefficient C_m and yaw moment coefficient C_n , the aerodynamic parameters are described in the following equations.

$$\begin{cases} C_l = C_{l0}(1+\Delta C_l) \\ C_m = C_{m0}(1+\Delta C_m) \\ C_n = C_{n0}(1+\Delta C_n) \end{cases} (8)$$

where C_{l0} , C_{m0} , C_{n0} are the rolling moment, pitching moment coefficient and yaw moment coefficient in the nominal aerodynamic model.

The inner loop model with parameter variation can be obtained:

$$\begin{cases} \dot{x}_2 = f_2(x_2) + \overline{f}_t(x_2) + g_2(x_2)u \\ y = C_2 x_2 + Ff \end{cases} (9)$$

where $\overline{f}_t(x_2)$ is the coupling moment term of inner loop nonlinear dynamics caused by parameter variation.

The rolling moment , pitching moment and yaw moment will change due to variation from equations (1), (2) and (7), they will affect the angular velocity signal, increase the error with the inner loop angular velocity fault state in the equation, and lead to the deterioration of the fault diagnosability evaluation accuracy.

III. FAULT DIAGNOSABILITY EVALUATION SCHEME

In this section, the diagnosability quantitative evaluation algorithm based on JS divergence and AKDE is proposed through strict mathematical derivation and proof.

A. Design of fault diagnosability index

For the F-16 inner loop control system, the residual is generated by the error between the actual output signal y of the flight control system and the observed signal $\hat{y}$. The output residual of the system (9) can be expressed as

$$r = y - \hat{y} \quad (10)$$

Theoretically, if the fault is diagnosable, the PDF of the residual *r* deviates from zero, it means that the fault can be diagnosed. For different forms of faults, their corresponding residual probability density functions are also different. However, considering the influence of parameter variation in the flight control system, the PDF of the residual *r* do not equal zero when the system is normal. At the same time, with the help of distance similarity distributed by multiple probabilities, the similarity and difference of faults can be measured, so as to achieve the purpose of quantitatively evaluating the fault diagnosability of dynamic systems.

The log likelihood function is introduced:

$$\lambda(r) = \log \frac{p_i(r)}{p_{NF}(r)} \quad (11)$$

According to the logarithmic characteristic of (11), when fault f_i occurs and can be detected, the PDF of the sensor output residual satisfy $p_i(r) > p_{NF}(r)$, and the likelihood function satisfy $E\left[\lambda(r)\right] > 0$, which can reflect the degree to which the system output is affected. The expression is:

$$E\left[\lambda(r)\right] = E\left[\log \frac{p_i(r)}{p_{NF}(r)}\right] \quad (12)$$

We find that (12) satisfies the calculation formula:

$$K(p_i \parallel p_{NF}) = \int_{-\infty}^{+\infty} p_i(r) \log \frac{p_i(r)}{p_{NF}(r)} dr = E_{p_i}\left[\log \frac{p_i(r)}{p_{NF}(r)}\right] \quad (13)$$

In order to make up for the asymmetry of KLD and define the evaluation scale of fault diagnosability, this paper measures fault diagnosability through JS divergence. Set

$$m_i = \frac{1}{2}(p_i + p_{NF}) \quad (14)$$

Based on (13) and (14), it can be deduced that

$$\begin{aligned} J(p_i \parallel p_{NF}) &= \frac{1}{2}K(p_i \parallel m_i) + \frac{1}{2}K(p_{NF} \parallel m_i) \\ &= \frac{1}{2}\int_{-\infty}^{\infty} p_i(r) \log\left(\frac{2p_i(r)}{p_i(r)+p_{NF}(r)}\right) dr \\ &+ \frac{1}{2}\int_{-\infty}^{\infty} p_{NF}(r) \log\left(\frac{2p_{NF}(r)}{p_i(r)+p_{NF}(r)}\right) dr \end{aligned} \quad (15)$$

Since the JS divergence minimization of both PDF $p_i(r)$ is equivalent to the maximum likelihood estimation of them, the fault diagnosability $FD(f_i)$ is defined as

$$FD(f_i) = \min\left[J(p_i \parallel p_{NF})\right] \quad (16)$$

On account of the properties of (15), $FD(f_i) \in (0,1)$. JS divergence is adopted as an index to measure the similarity of two different probability distributions. When the fault occurs, the sensor output residual state in the normal system is taken as a reference distribution, and the smaller the value of $FD(f_i)$, the higher the similarity between the practical distribution and the reference distribution, which means that the fault f_i is less difficult to diagnose. When $FD(f_i) = 0$, the fault f_i cannot be diagnosed; Conversely, the larger the value of $FD(f_i)$, the easier the fault f_i is to be diagnosed.

It is difficult to obtain the accurate solution of (16) because the nonlinear factors are contained in the system. Even after solving the PDF of residual, it still faces the problem of high computational complexity. Therefore, Monte Carlo (MC) is used to solve the problem. MC refers to the process of randomly extracting values from the input probability distribution through pseudo-random numbers. Any given sample may fall at any position within the input distribution range [9], [10].

$$\hat{J}(p_i \parallel p_{NF}) = \frac{1}{n_s}\sum_{i=1}^{n_s}(\log\frac{2\hat{p}_i(r)}{\hat{p}_i(r)+\hat{p}_{NF}(r)} + \frac{1}{n_a}\sum_{i=1}^{n_a}\log\frac{2\hat{p}_{NF}(r)}{\hat{p}_i(r)+\hat{p}_{NF}(r)}) \quad (17)$$

where n_s is the number of samples $\hat{p}_i$ from p_i and n_a is the number of samples $\hat{p}_{NF}$ from the PDF p_{NF}. The evaluated error of (18) obeys a normal distribution whose expectation is zero and variance is

$$\sigma_m^{\ 2} = \frac{1}{n_s}\left(E\left[\log(\frac{2\hat{p}_i(r)}{\hat{p}_i(r)+\hat{p}_{NF}(r)})\right]^2\right) + \frac{1}{n_a}\left(E\left[\log(\frac{2\hat{p}_{NF}(r)}{\hat{p}_i(r)+\hat{p}_{NF}(r)})\right]^2\right) \quad (18)$$

It can be obtained that the evaluated error obtained by MC obeys $e_M \sim N(0,\sigma_m^2)$ of samples is selected, the smaller the error between the JS divergence calculated by MC and the value calculated by (17), also the more accurate the diagnostic evaluation result will be.

B. Adaptive kernel density estimation of residuals

In order to calculate the fault diagnosability $FD(f_i)$, we must know the PDF of p_i and p_{NF}. A group of observed random variables from an unknown distribution function is mainly used in KDE. For the problem of estimating the unknown PDF of p_i and p_{NF}, the prior knowledge about the distribution is not utilized and the certain mathematical form of PDF is not required in KDE which is a prediction estimation that only uses the sample data itself [11].

Suppose $R_1, R_2, \cdots, R_n$ are independent identically distributed samples extracted from the output residual R of the one-dimensional population system and R has an unknown density function $p(r)$, $r \in R$, then the kernel density $p(r)$ is estimated as

$$\hat{\varphi}(r) = \frac{1}{nh}\sum_{i=1}^{n}K_r(\frac{r-R_i}{h}) \quad (19)$$

where $\hat{\varphi}(r)$ represents the estimation of the PDF, n is the number of samples, h is the global bandwidth of the sampling point, $K_r(r)$ is the kernel function, and R_i is the sampling point.

In this paper, the typical Gaussian kernel is selected as the kernel function because it has higher accuracy for the NKDE and its functional formula is

$$K_r(\frac{r-R_i}{h}) = \frac{1}{2\pi}e^{-\frac{|r-R_i|^2}{2h^2}} \quad (20)$$

According to (20), KDE is not only related to the sample size n, but also to the selection of kernel function $K_r(r)$ and bandwidth h. On the premise that the sample has been determined, once the appropriate h is determined, the kernel method can be used to better approximate the real PDF. If the assumed value h is large, it will submerge the details of the density, making the density estimation curve too smooth, which leads to the coverage of important features; On the contrary, it will show unimportant random details, resulting in greater fluctuation of density estimation and poor stability. Therefore, the choice of bandwidth is very important to KDE. AKDE is a density estimation method that adapts the bandwidth to sample data, and reduces the impact of data outliers on the overall estimation by changing the bandwidth.

The parameter adaptive law h is set:

$$h_i = h\eta_i \quad (21)$$

where h_i is the bandwidth calculated for the sampling point R_i and η_i can be obtained by the following formula:

$$\eta_i = \left\{\frac{\tilde{\varphi}(R_i)}{\vartheta}\right\}^{-a} \quad (22)$$

where a is a non negative constant, $\tilde{\varphi}(R_i)$ is the preliminary estimation of the probability density at the sampling point R_i, ϑ is the geometric average of the probability density of n sampling point, and is expressed as

$$\log(\vartheta) = \frac{1}{n}\sum_{i=1}^{n}\log\tilde{\varphi}(R_i) \quad (23)$$

$\tilde{\varphi}(R_i)$ is evaluated by the initial bandwidth obtained by the fixed h_0.

KDE can be realized by selecting appropriate parameters h, h_0, a. a is performed based on the maximum likelihood criterion, and $h_0 = h$ is chosen as a preliminary estimate. The rule of thumb (ROT) is usually used to determine the optimal h. However, due to the strong randomness of the sample data, h is too smooth for non unimodal distribution. It is recommended to slightly reduce the value of bandwidth (21) as compensation:

$$h = 0.9 \min\left(\hat{\sigma}, \frac{IQR}{1.34}\right) n^{-1/5} \quad (24)$$

where $\hat{\sigma}$ represents the standard deviation of the sample, IQR denotes the interquartile range.

The probability of each sampling point is estimated through AKDE from the sampling point excluding itself. The probability at each sampling point can be calculated as

$$\tilde{\varphi}^*(R_i) = \frac{1}{(n-1)} \sum_{j=1, j\neq i}^{n} \frac{1}{h_j} K_r\left(\frac{R_i - R_j}{h_j}\right) \quad (25)$$

where $\tilde{\varphi}^*(R_i)$ is the probability of sampling points R_i given other $n-1$ sampling points.

By combining the proposed bandwidth selection method, the shape of the traditional PDF can be changed, which better describes the PDF of the system residual p_i, p_{NF} under fault and normal conditions.

IV. Simulation Verification

In this section, simulations have been implemented to assess the above fault diagnosability evaluation result based on the Matlab/Simulink simulation platform.

A. Analysis of simulation results

The initial state of the flight is shown in Table I. Based on reference signal, the fixed-roll-angle post-stall pitch maneuver is completed and $\beta_d = 0\,\text{deg}$. The nominal NDI controller parameters are selected as $k_p = k_d = k_r = 10$, $k_\alpha = k_\beta = k_\varphi = 2$. The initial state of the flight is set in Table I. The simulation time is 20s, and the simulation step is 0.1s. The Fault matrix F_1, F_2 are set as: $F_1 = \begin{bmatrix}1 & 0 & 0\end{bmatrix}^T$, $F_2 = \begin{bmatrix}0 & 1 & 0\end{bmatrix}^T$. The sensor fault $f(t)$ is set as:

$$f(t) = \begin{cases} 0 & t < 4 \\ 2\sin(2\pi t) & 4 \le t < 12 \\ 4\sin(2\pi t) & t \ge 12 \end{cases} \quad (26)$$

TABLE I. Initial State of the Flight

Parameters	*Value*	*Parameters*	*Value*
x_0	$0m$	θ_0	$0\,\text{deg}$
y_0	$0m$	α_0	$0\,\text{deg}$
z_0	$3000m$	β_0	$0\,\text{deg}$
V_0	$125m/s$	φ_0	$0\,\text{deg}$
ψ_0	$0\,\text{deg}$	p_0, q_0, r_0	$0\,\text{deg}/s$

The simulation results of fault detection in two fault cases are given below. As shown in Fig. 1, when the system is normal, the observer can largely suppress the influence of aerodynamic parameter variation, and the residual r_1, r_2 is very small. When the roll angle sensor fault f_1 occurs in 4s, r_1 increases obviously; And with the amplitude of time-varying fault increasing in 12s, the deviation amplitude increases. Also, when the pitch angular velocity sensor f_2 fails, r_1 has a analogous trend. In addition, compared with the residual r_1 corresponding to the fault f_1, residual r_2 is smaller. On the basis of the residual response results, it can be proved qualitatively that both faults can be effectively diagnosed, and the diagnosability of the roll angle sensor fault f_1 is greater than that of the pitch angle sensor fault f_2.

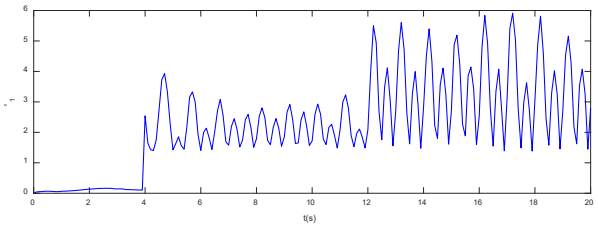

(a) Comparison curves of roll rate p

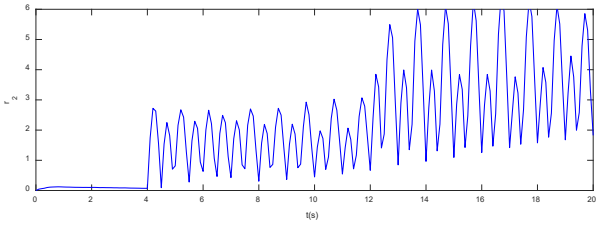

(b) Comparison curves of pitch rate q

Fig. 1. Residual response curve of fault detection.

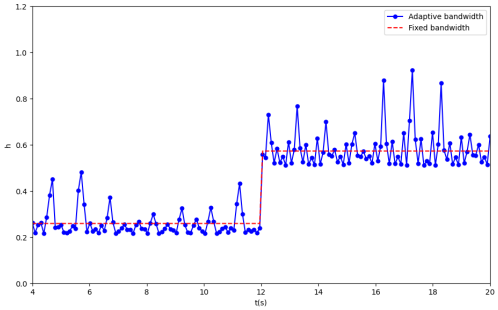

(a) Comparison curves of roll rate p

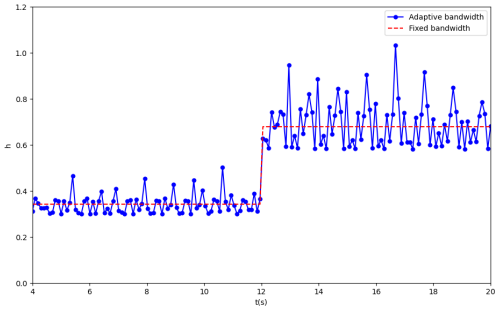

(b) Comparison curves of pitch rate q

Fig. 2. Residual probability density function bandwidth curve.

The comparison curves of adaptive bandwidth calculation results are shown in Fig. 2. The solid blue line is the curve for calculating the bandwidth according to (21), and the broken red line is acquired through (24). When the fault occurs in the roll angular velocity sensor at the 4s, the fixed

bandwidth is 0.2600. When the fault amplitude increases at 12s, the fixed bandwidth increases to 0.5738, while the adaptive bandwidth shows a certain fluctuation around the fixed bandwidth, reflecting the individuality of the residual. When the pitch angle sensor fails, the fixed bandwidth of the two periods is calculated as 0.3430 and 0.6798.

As shown in Fig. 3, the estimation of angular velocity sensor residual PDF based on adaptive bandwidth is basically consistent with the actual sample data distribution. The local adaptability of the fixed bandwidth KDE is poor and the distribution curve is relatively smooth, while AKDE can more specifically display the local characteristics and more accurately simulate the stochastic characteristics.

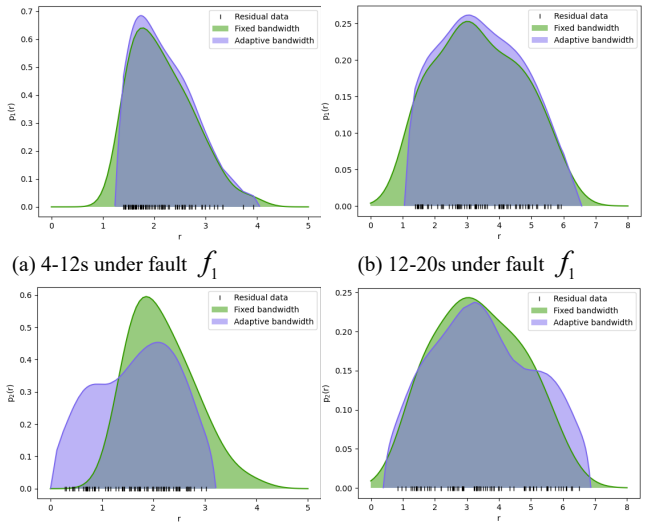

(a) 4-12s under fault f_1 (b) 12-20s under fault f_1

(c)4-12s under fault f_2 (d) 12-20s under fault f_2

Fig. 3. Residual probability density function estimation curve.

The fault diagnosability is presented in Table. II. When the sensor is normal, The fault diagnosability. $FD(f_1)$ and $FD(f_2)$ are very small because the fault has not yet occurred, however, due to the tracking error and system disturbance of the observer in the initial stage, there exists a certain deviation from zero. When the F-16 angular velocity sensor starts to malfunction at 4s, the fault diagnosability increases significantly, and $FD(f_1)$ is slightly larger than $FD(f_2)$, which indicates that both can be diagnosed, and f_2 is more difficult to diagnose than f_1 to some extent; The fault amplitude of the same channel starts to increase at 12s, the diagnosability of both f_1 and f_2 is greatly enlarged compared with the period of 4-12s, which are consistent with the analysis of simulation curve in Fig. 1.

TABLE II. FAULT DIAGNOSABILITY COMPARISON

Fault location	***0-4s***	***4-12s***	***12-20s***
Roll angular velocity	0.1691	0.6362	0.8890
Pitch angular velocity	0.1934	0.4276	0.6248

So far, for the complex flight control system with high maneuverability, it can prove that the quantitative fault diagnosability evaluation method based on AKDE-JS proposed in this paper can accurately evaluate the diagnosability of different types and sizes of fault by simulation experiments and analysis.

V. CONCLUSION

A quantitative evaluation method of fault diagnosability based on AKDE-JS for F-16 fighter is reported in this paper. The KDE bandwidth adaptive law is set by the PDF geometric mean of the residual data sampling points, which can more exactly reflect the characteristics of the individual residual data; Based on Monte Carlo, the KDE that obeys the Gaussian probability distribution when the system is normal and the JS divergence of PDF estimated according to the residual are calculated to quantitatively evaluate the fault diagnosability. Finally, the rationality of the method proposed in this paper is verified by simulation experiments. The obtained probability density curve of sensor fault output residual fits the actual distribution better, and the evaluation result is more accurate.

It is worth noting that the current work is a preliminary study on the fault diagnosability of the F-16 fighter. The following issues will be discussed in the future work:

- The work approximates the JS divergence of the two distributions through Monte Carlo, however there are still small error terms in the calculation results. How to simplify the calculation complexity of nonlinear structures will be further studied in the future.

ACKNOWLEDGMENT

The authors gratefully acknowledge the financial supports by the National Science Foundation of China under Grant numbers 62173179.

REFERENCES

[1] D. Zhai, L. An, X. Li, and Q. Zhang, “Adaptive fault-tolerant control for nonlinear systems with multiple sensor faults and unknown control directions,” IEEE Transactions on Neural Networks Learning Systems, pp. 1–11, 2017.

[2] F. Stoican, F. Petzke, I. Prodan, and S. Streif, “Hierarchical control with guaranteed fault diagnosability,” IFAC-PapersOnLine, vol. 51, no. 24, pp. 1105–1110, 2018.

[3] Z. Xing and Y. Xia, “Evaluation and design of actuator fault diagnosability for nonlinear affine uncertain systems with unknown indeterminate inputs,” International Journal of Adaptive Control and Signal Process□ing, vol. 31, 2017.

[4] D. Jiang and W. Li, “Permissible area analyses of measurement errors with required fault diagnosability performance,” Sensors, vol. 19, no. 22, pp. 4880–, 2019.

[5] J. Stiefelmaier, A. Gienger, M. Bx00F6;hm, O. Sawodny, and C. Tarx00ED;n, “Sensor placement for qualitative fault diagnosability in large-scale adaptive structures,” in 2021 International Conference on Mechatronics, Robotics and Systems Engineering (MoRSE), pp. 1–6, 2021.

[6] K. Yuan, X. Cheng, Z. Gui, F. Li, and H. Wu, “A quad-tree-based fast and adaptive kernel density estimation algorithm for heat-map generation,” International Journal of Geographical Information Science, vol. 33, no. 12, pp. 2455–2476, 2019.

[7] H. Song, C. Sun, C. Zhang, and T. Ren, “The fault diagnosis of gear based on kernel density estimation,” Journal of Computational Methods in Sciences and Engineering, vol. 18, no. 3, pp. 779–791, 2018.

[8] J. Pan, W. He, Y. Shi, R. Hou, and H. Zhu, “Uncertainty analysis based on non-parametric statistical modelling method for photovoltaic array output and its application in fault diagnosis,” Solar Energy, vol. 225, pp. 831–841, 2021.

[9] X. Zhang, C. Delpha, and D. Diallo, “Jensen-shannon divergence for non-destructive incipient crack detection and estimation,” IEEE Access, vol. 8, pp. 116 148–116 162, 2020.

[10] Z. Li, X. Bai, R. Hu, and X. Li, "Measuring phase-amplitude coupling based on the jensen-shannon divergence and correlation matrix," IEEE Transactions on Neural Systems and Rehabilitation Engineering, vol. 29, pp. 1375–1385, 2021.

[11] X. Wu, "Robust likelihood cross-validation for kernel density estimation," Journal of Business Economic Statistics, vol. 37, no. 4, pp. 761–770, 2019.